Physica B 481 (2016) 8–18

Contents lists available at ScienceDirect

Physica B

journal homepage: www.elsevier.com/locate/physb

Time-resolved luminescence from quartz: An overview of contemporary developments and applications

M.L. Chithambo [a,*], C. Ankjærgaard [b], V. Pagonis [c]

[a] Department of Physics and Electronics, Rhodes University, PO BOX 94, Grahamstown 6140, South Africa
[b] Soil Geography and Landscape Group, Wageningen University Netherlands Centre for Luminescence Dating, Droevendaalsesteeg 3, 6708 PB Wageningen, The Netherlands
[c] McDaniel College, Physics Department, Westminster, MD 21157, USA

ARTICLE INFO

Article history:
Received 30 March 2015
Received in revised form
12 August 2015
Accepted 9 October 2015

Keywords:
Time-resolved optical stimulation
Luminescence lifetimes
Quartz
Feldspar

ABSTRACT

Time-resolved optical stimulation of luminescence has become established as a key method for measurement of optically stimulated luminescence from quartz, feldspar and α-Al_2O_3:C, all materials of interest in dosimetry. The aim of time-resolved optical stimulation is to separate in time the stimulation and emission of luminescence. The luminescence is stimulated from a sample using a brief light pulse and the emission monitored during stimulation in the presence of scattered stimulating light or after pulsing, over photomultiplier noise only. Although the use of the method in retrospective dosimetry has been somewhat limited, the technique has been successfully applied to study mechanisms in the processes leading up to luminescence emission. The main means for this has been the temperature dependence of the luminescence intensity as well as the luminescence lifetimes determined from time-resolved luminescence spectra. In this paper we review some key developments in theory and applications to quartz including methods of evaluating lifetimes, techniques of evaluating kinetic parameters using both the dependence of luminescence intensity and lifetime on measurement temperature, and of lifetimes on annealing temperature. We then provide an overview of some notable applications such as separation of quartz signals from a quartz–feldspar admixture and the utility of the dynamic throughput, a measure of luminescence measured as a function of the pulse width. The paper concludes with some suggestions of areas where further exploration would advance understanding of dynamics of luminescence in quartz and help address some outstanding problems in its application.

1. Introduction

Time-resolved optical stimulation (TR-OSL) is a key method for measurement of optically stimulated luminescence that relies on the use of repetitive light pulses of constant intensity to separate in time the stimulation and emission of luminescence. The luminescence is stimulated using a brief light pulse during which the measured signal comprises a monotonically increasing luminescence component and constant scattered stimulating light. After the pulse, the luminescence is measured over a background of photomultiplier noise only and decreases in intensity with time.

There are several advantages of time-resolved optical stimulation over steady-state stimulation. The method is capable of high signal-to-noise ratio over extended measurement times [1]. In addition, pulsing rather than continuous optical stimulation means that only a negligible proportion of the optically stimulable charge is sampled thereby enabling repeated monitoring of the luminescence without an appreciable loss in intensity. Time-resolved optical stimulation provides a means to measure luminescence lifetimes. The lifetimes are associated with charge transfer processes within the phosphor and as such help to better explain the luminescence emission process.

The first measurements of time-resolved luminescence from materials of interest in retrospective dosimetry were first reported by Sanderson and Clark [2] on feldspar stimulated with 470 nm light using a 10 ns pulse. The study showed evidence of luminescence lifetimes of the order of hundreds of nanoseconds. The method was then used to investigate luminescence processes from α-Al_2O_3:C, a luminescence dosimeter [3–6]. Further studies on pulsed luminescence from feldspars were then reported by Clark et al. [7] and Clark and Bailiff [8] using an 850 nm pulsed laser. The first measurements of TR-OSL from quartz, a common natural dosimeter, independently reported by Bailiff [9] using a 470 nm pulsed laser system and by Chithambo and Galloway [1] using a pulsed 525 nm green LED system, showed a principal luminescence lifetime of about 40 μs from this material. Later work

* Corresponding author. Fax: +27 466038757.
E-mail address: m.chithambo@ru.ac.za (M.L. Chithambo).

http://dx.doi.org/10.1016/j.physb.2015.10.014
0921-4526/

showed the presence of shorter subsidiary lifetimes in quartz depending on certain combinations of annealing and measurement temperature [9–12] as well as on the thermal provenance of the quartz [13]. The method has also been widely used to study dynamics of luminescence in quartz e.g. [9–15], to develop a kinetic model of pulsed OSL in quartz [16] and applied in retrospective dosimetry [17, 18].

The aim of this paper, which is not meant to be exhaustive, is to present a review of some contemporary developments in the theory and applications of time-resolved optical stimulation of luminescence in quartz. The paper looks at instrumentation, discusses luminescence lifetimes and luminescence intensity and their use in evaluating kinetic parameters, presents an overview of models for time-resolved luminescence, summarises some notable applications of the method and concludes with an outlook of areas where further work would advance understanding of mechanisms of luminescence in quartz and help refine its applications.

2. Measurement techniques

There are several methods for measurement of time-resolved or pulsed optically stimulated luminescence (POSL) that have been reported but in this section we reflect only on two, time-correlated photon counting and the other, a time-tag technique.

2.1. Time-correlated photon counting

The stimulation of luminescence in this method may be discussed with reference to the schematic diagram of Fig. 1 which shows a light pulse of duration t_w. Luminescence is emitted both during and after the light pulse. Since the luminescence photons emitted during and after optical stimulation using a single light pulse are not sufficient for reliable statistical analysis, it is often necessary to build up a time-resolved luminescence spectrum by summing spectra from several scans or sweeps. In this case, the total measurement time known as the on-time t_{ON} is the product of the pulse width (i.e. the duration of the light pulse) and the number of sweeps. The data points displayed as a function of time in the time-resolved luminescence spectrum measured in this manner are not separated in time contiguously as in a conventional OSL decay curve. The data points are arranged depending on their correlation in time with the luminescence stimulating light pulse. The correlation in time between the light pulse and the resultant luminescence photon is determined by a multichannel scaler e.g. see Refs. [19, 20]. The multichannel scaler records the number of events (detection of luminescence photons) that occur during the time interval t_i to $t_i+\Delta t$ as a function of time where Δt is the dwell time (Fig. 1). The measurement time per sweep or dynamic range t which need not be equal to the period P is quantized into an integral number of channels each of duration Δt by the relation $t=n\Delta t$ where n is the channel or bin number.

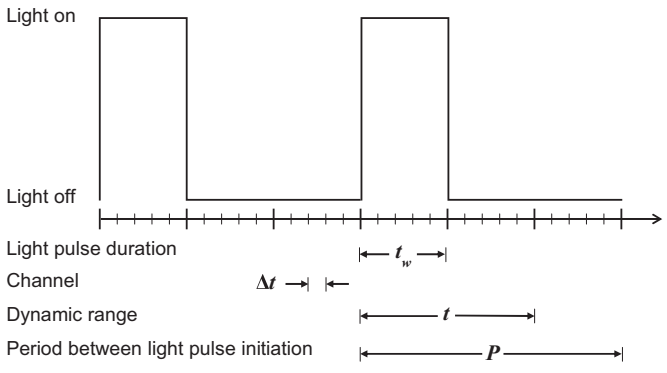

Fig. 1. A schematic diagram of a luminescence stimulating light pulse of duration t_w and period P. The dynamic range t is subdivided into an integral number of $n\Delta t$ channels [20].

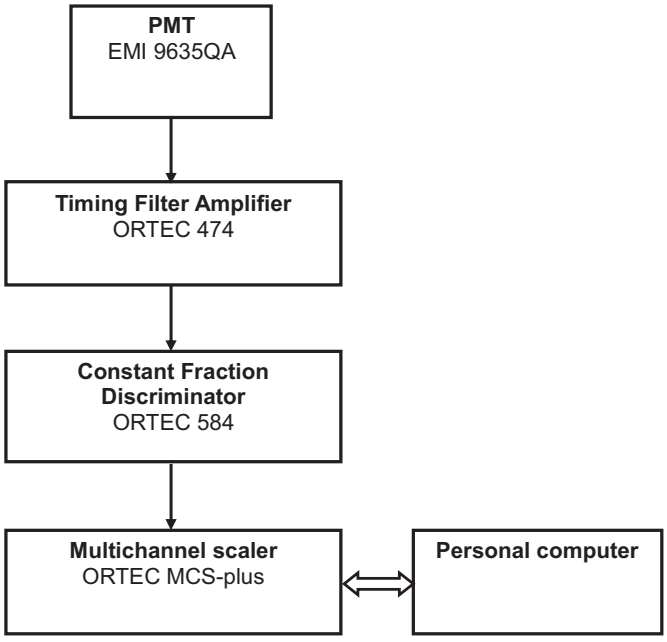

Fig. 2. A schematic diagram of the pulsing system showing the arrangement for detection and measurement of time-resolved luminescence spectra [20].

Fig. 2 shows a schematic diagram of the luminescence detection assembly for a typical pulsing system [19]. The luminescence is detected by the photomultiplier tube (EMI 9635QA) whose signals are amplified by the timing filter amplifier (Ortec 474) and then counted by the constant fraction discriminator (Ortec 584). The multichannel scaler (EG & G Ortec MCS-plus™) triggers a set of light-emitting diodes as well as initiates a data-recording sweep in the computer. Once the sweep is started the multichannel scaler records photon counts sequentially in its memory with no dead-time either between channels or at the end of each sweep. The time-resolved luminescence spectrum measured in this way is a plot of cumulative photon counts against time for the dynamic range selected. An example of a time-resolved luminescence spectrum is shown in Fig. 3. The spectrum was measured from a

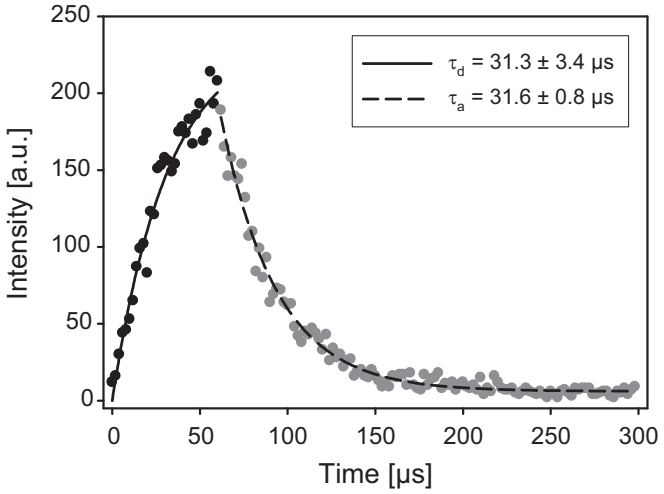

Fig. 3. Time-resolved luminescence from sedimentary quartz measured using a 60 μs pulse over a dynamic range of 300 μs and 10^6 sweeps following a beta dose of 7 Gy [21]. The parameters τ_a and τ_d are discussed later in the text.

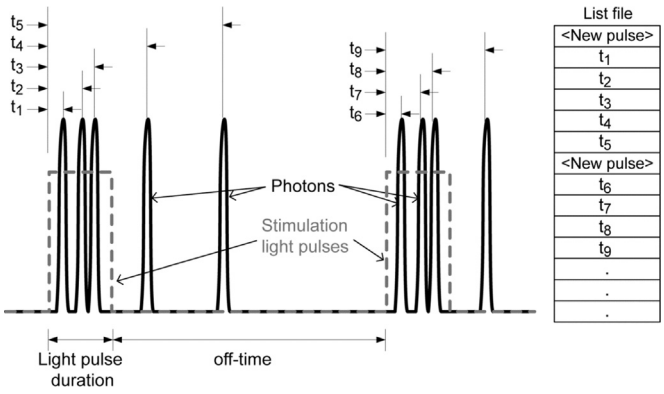

Fig. 4. Diagram showing the principle of single-photon time-stamping with the list on the right showing the sequential listing of time-stamping events. Redrawn after Lapp et al. [24]. Note that the duration of the stimulation pulse is also referred to in some reports as the *on*-time e.g [24].

sample of quartz irradiated to 7 Gy over 10^6 sweeps at 60 μs pulse width per sweep [21]. The significance of the solid lines through data and the parameters τ_a and τ_d will be explained later in the text.

The development and design of measurement systems for this mode of measurement have been reported by Chithambo and Galloway [1] and Chithambo [19, 20]. The method has also been used by Pagonis et al. [16].

2.2. Time-tag mode

The time-stamp or time-tag method, was initially introduced by Becker and Hickl in 1996 [22] and used for its large potential in single molecule spectroscopy when sufficiently fast computers with large memory capacity became available e.g. [22, 23]. The 'time-stamp' mode is a photon counting technique where the arrival of every emitted photon above a certain threshold is time-stamped with respect to the beginning of the preceding stimulation light pulse contrary to building up photon distributions (see Section 2.1). The principle of photon time-stamping is illustrated in Fig. 4 for two consecutive pulses of stimulation light. At the beginning of each stimulation light pulse, a time marker is inserted in a list file shown to the right in Fig. 4. The time of arrival of the luminescence photons during and after the stimulation pulses are each sequentially recorded in the list file with respect to the time marker [22, 24]. The time stamping is continued for several thousands of stimulation pulses (the total stimulation time) as luminescence emission is a rather inefficient process emitting typically only a few photons per pulse, and the resulting data are written into a first-in-first-out (FIFO) buffer. The output of the FIFO is continuously read by a computer, resulting in a continuous long 1-D string of arrival time data, often with a file size in the gigabytes range.

The first prototype photon time-stamp system for use in luminescence dosimetry was developed as an attachment for the commercially available Risø TL/OSL-DA luminescence measurement reader, enabling the adjustment of LED pulse durations and periods between pulses (also termed *on*- and *off*-times) to between 2 μs to 10 ms, and a time resolution down to 18 ns [17, 18]. The pulsed attachment was later made more flexible to include LED pulse *on*- and *off*-times from 0.2 μs to 9.9 s, and further implementing a commercially available *ORTEC 9353 Time Digitizer* board with a time resolution of 100 ps [24]. Both Denby et al. [17] and Lapp et al. [24] described the possibility of gating the pulsed luminescence signal, such that only photon pulses detected during a pre-set gating window relative to the diode pulse are passed on to the photon counter. For the Risø TL/OSL-DA system, this gating period can only be specified within the period between pulses (the *off*-time), and does not operate in time-stamping mode but records the data as an ordinary POSL decay curve as a function of stimulation time in a number of pre-determined bins [17, 24].

3. Models of time-resolved luminescence

There are two models for TR-OSL in quartz, a phenomenological model reported by Chithambo [21, 25] and a kinetics model developed by Pagonis et al. [16]. The two models produce equivalent results although their description of the luminescence process is not identical. The main features of the model by Chithambo [21, 25] are presented in Sections 3.1 through 4. The kinetics model of Pagonis et al. [16] and related further developments are described in Sections 5.2 and 5.3.

3.1. Phenomenological model of Chithambo [21, 25]

In this description, we consider a simple case consisting of one electron trap with an initial electron population A and one kind of recombination centre. If the probability of stimulation per unit time from the trap is s, and the decay constant giving the probability per unit time that a stimulated electron will produce luminescence is λ, then the rate of change of the number N of stimulated electrons during stimulation, can be expressed as

$$\frac{dN}{dt} = sA - \lambda N. \tag{1}$$

Eq. (1) can then be used to formulate equations that describe the time-dependence of the luminescence during and after stimulation, and hence the luminescence lifetime as well as the luminescence throughput.

3.1.1. Luminescence lifetimes

Lifetimes can be evaluated from either the portion of a time-resolved luminescence spectrum after the pulse by fitting exponential functions of the form

$$f(t) = A\exp(-t/\tau) + B \tag{2}$$

or from the portion during the light pulse by fitting functions of the form

$$f(t) = sA[1 - \exp(-t/\tau)] \tag{3}$$

where τ is the lifetime, t is time, A is a scaling parameter and B is a constant added to account for the background [21, 25]. An example of such plots is shown in Fig. 3 where the solid lines through data during and hyphenated lines after the light pulse, giving respective lifetimes $\tau_d = 31.3 \pm 3.4$ μs and $\tau_a = 31.6 \pm 0.8$ μs are the best fits of Eqs. (3) and (2). The error $\Delta\tau$ in the lifetime reflects the scatter in data in the TR-OSL spectrum used to evaluate the lifetime. The lifetimes extracted from either portion of the time-resolved luminescence spectrum are expected to be similar since the recombination mechanism responsible for emitted luminescence is the same both during and after stimulation [21, 25].

The simple model consisting of one electron-trap and one type of luminescence centre with emission involving electron transition through the conduction band is similar to the discussion of OSL by McKeever and Chen [26] and Chen and Leung [27]. As noted previously [21, 25], in typical time-resolved optical stimulation, the stimulating light pulse is brief and consequently, the reduction in trapped charge due to optical stimulation in that time is negligible and as a result retrapping is also assumed to be negligible. The theoretical bases of mathematical methods for analysis of time-resolved luminescence spectra, including non-first order cases,

have otherwise been described in greater detail by Chithambo [25] and compared with experimental and computer-simulated results [21].

Experimentally, the lifetime as measured from quartz using the instrumentation described earlier in Section 2 denotes the delay between stimulation and emission of luminescence [1, 19, 20]. In terms of dynamics, the luminescence lifetimes may be associated with three possible physical mechanisms, namely, the time required to stimulate an electron from a trap, the transit time through the conduction band and the lifetime of the excited state at the recombination centre but in most cases, the dominant component is the relaxation time at the luminescence centre ([28] and references therein).

4. Evaluation of kinetic parameters

The probability of luminescence emission from the excited state of a luminescence centre depends on temperature [29]. Time-resolved optical stimulation can be used to evaluate some kinetic parameters associated with the physical processes of luminescence emission through the dependence of lifetimes and luminescence intensity on temperature. The information available in this way includes the activation energy of thermal assistance E_a, the activation energy of thermal quenching ΔE and the frequency factor for the thermal quenching process ν. We summarise below some of the key techniques for obtaining these parameters.

4.1. Calculations using dependence of lifetimes on measurement temperature

Fig. 5 shows a typical dependence of lifetimes on measurement temperature. In this example, the measurements were made on sedimentary quartz irradiated to 75 Gy and stimulated using 525 nm LEDs. Lifetimes are constant at about 40 μs between 20 and 100 °C and then decrease thereafter to about 7 μs at 200 °C. The profile of lifetimes against temperature in Fig. 5 is independent of whether the sequence of measurements is made with the temperature increasing or decreasing [14, 28]. The thermal effect of the stimulation temperature on lifetimes can be described as

$$\tau(T) = \tau_{rad}/[1 + C\exp(-\Delta E/kT)] \quad (4)$$

where τ_{rad} is the radiative lifetime at 0 K, ΔE is the activation energy of thermal quenching, k is Boltzmann's constant and C is a dimensionless constant where $C=\nu\tau_{rad}$. In this example, the activation energy ΔE for thermal quenching and dimensionless constant C are equal to 0.66 ± 0.05 eV and 4×10^7 respectively. Typical values of ΔE reported for quartz include 0.64 eV from radioluminescence [30], 0.78 eV from thermoluminescence [31], and 0.79 eV by CW-OSL [32].

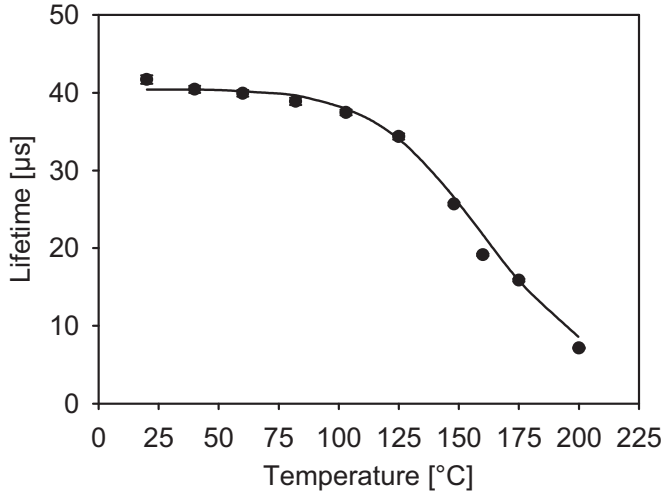

Fig. 5. The change in luminescence lifetimes with temperature for quartz irradiated to 75 Gy and pulse-stimulated at 525 nm (reproduced from [14]).

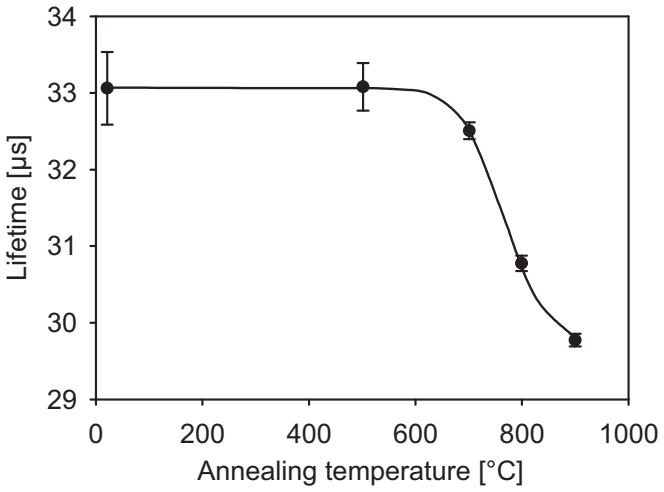

Fig. 6. The influence of annealing temperature on luminescence lifetimes for measurements made at 20 °C [12].

4.2. Calculations using dependence of lifetimes on annealing temperature

When quartz is annealed beyond its first phase inversion temperature of 570 °C, the sensitivity of its optically stimulated luminescence increases beyond that observed at room temperature and in particular shows significant changes near its phase inversion temperatures of 570 and 870 °C [10, 33, 34]. It is now also known that annealing affects not only the sensitivity but also luminescence lifetimes in quartz [10, 12].

Fig. 6 shows the dependence of lifetimes on annealing temperature for natural quartz annealed up to 900 °C. In this example, lifetimes are constant at about 33 μs up to about 600 °C and then decrease gradually to about 29 μs when the annealing temperature is increased to 900 °C. The change with temperature of lifetime from a higher value τ_H to a lower one τ_L with annealing temperature is modelled as

$$\tau(T) = \tau_L + (\tau_H - \tau_L)/[1 + C\exp(-W/kT)] \quad (5)$$

where C is the dimensionless constant described earlier, k is Boltzmann's constant, T is the absolute temperature and W is the activation energy above the valence band of the luminescence centre from which holes involved in the luminescence process are thermally released [10]. In this example, the value obtained for W is equal to 2.14 ± 0.01 eV and can be compared with 1.4 ± 0.4 eV reported by Galloway [10] or the range 1.34–1.55 eV given by Fleming [35]. Further, Fig. 6 also implies that annealing decreases the value of the dominant lifetime and, as is to be discussed, that it enhances the emission of luminescence from a particular recombination centre. This particular feature was examined in detail by Chithambo and Ogundare [15].

Although reports of similar studies in synthetic quartz are meagre, it is interesting to note that in synthetic quartz, annealing has a diametric effect to that shown in Fig. 6 and that as such it can be modelled as a shift in emission from τ_L to τ_H, that is, $\tau(T) = \tau_H + (\tau_L - \tau_H)/[1 + C\exp(-W/kT)]$ as shown by Chithambo et al. [36] who found $W=1.70 \pm 0.06$ eV in this case.

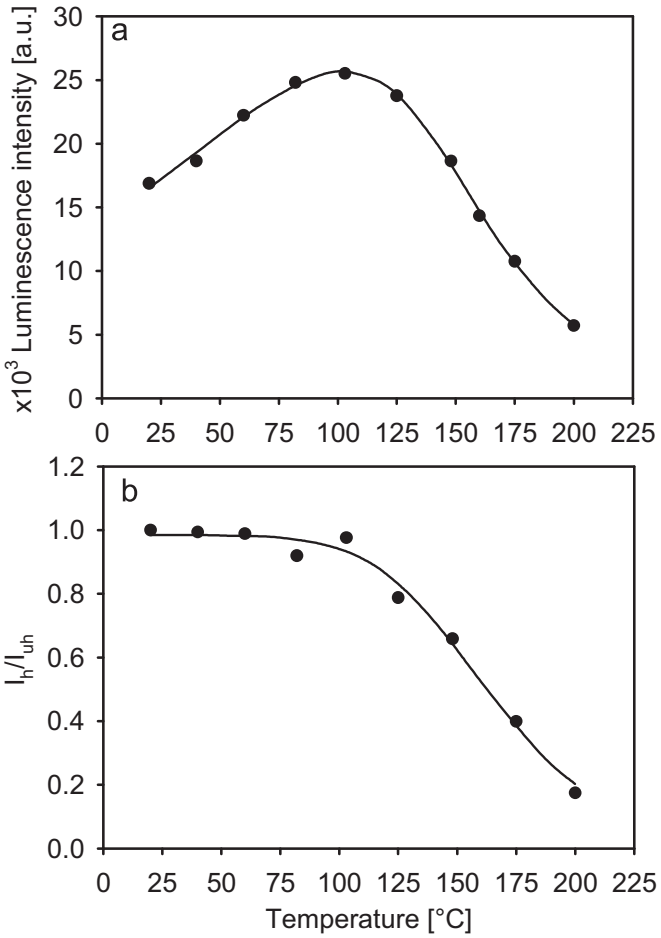

Fig. 7. (a) The change of luminescence intensity with measurement temperature for quartz irradiated to 75 Gy and pulse-stimulated at 525 nm [14] and (b) the ratio of intensities of luminescence stimulated from a sample under simultaneous heating and optical stimulation (I_h) to that under optical stimulation only (I_{uh}).

4.3. Calculations using luminescence intensity

There are two possible ways of evaluating kinetic parameters from the temperature dependence of luminescence intensity. These are discussed below with reference to Fig. 7.

In the measurement shown in Fig. 7(a), the luminescence intensity goes through a peak as a function of temperature. The behaviour shown is due to increasing thermal assistance to optical stimulation initially as the measurement temperature is increased between 20 and 100 °C, and from then on a decrease in intensity due to thermal quenching of the luminescence [14]. The overall change follows the relationship

$$I(T) = I_o \exp(-E_a/kT)/[1 + C \exp(-\Delta E/kT)] \quad (6)$$

where I_o is the initial value of the luminescence intensity, E_a is the activation energy for thermal assistance and all other symbols are as previously defined. Since the luminescence used in Eq. 6 can be integrated from the same spectra used in Eq. 4, the kinetic parameters in these two cases are complementary. In the example of Fig. 7, the value obtained for ΔE was 0.66 ± 0.05 eV which can be compared to 0.64 ± 0.03 eV obtained from Fig. 5.

If, on the other hand, the luminescence intensity decreases monotonically with measurement temperature, then a plot of the ratio of luminescence intensity measured at successively higher temperatures to that measured at constant temperature (Fig. 7(b)) can be described as

$$I(T) = I_o/[1 + C \exp(-\Delta E/kT)] \quad (7)$$

where all symbols have the same meanings as before [21, 28].

5. Modelling the luminescence process

5.1. Energy Band Model

In a study of the effect of annealing on luminescence lifetimes, Galloway [10] discussed his results in terms of a model previously used by Zimmerman [37] and Bøtter-Jensen et al. [33] to explain thermal sensitivity changes in quartz. In particular, the model of Bøtter-Jensen et al. [33] assumed the preferential capture of holes at non-radiative centres. A schematic diagram of the model of Galloway [10] built on that of Bøtter-Jensen et al. [33] is shown in Fig. 8 for natural quartz. The model retains the original assumption that annealing can cause a transfer of holes between a non-radiative recombination centre (R) and radiative recombination centres. In terms of time-resolved luminescence, a change in the value of lifetimes can be sufficiently explained by transfer of holes, through the valence band, between recombination centres (shown as L_H, L_L, L_S) with which lifetimes (say τ_H, τ_L, τ_S) are associated where $\tau_H > \tau_L > \tau_S$. For completeness, electrons traps are included consisting of shallow traps (ST), optically sensitive traps involved in optically stimulated luminescence (OST) and deep-traps which are not optically stimulated (DT). This model has been used to explain many features of time-resolved luminescence including the influence of annealing, preheating and duration of annealing on luminescence lifetimes [10–13, 15, 36].

5.2. A kinetic model for pulsed-OSL in quartz

Pagonis et al. [16] presented a kinetic model for pulsed OSL in quartz. The model quantitatively reproduces typical profiles of time-resolved luminescence spectra from quartz. As the authors point out, the model is not meant to exhaustively describe all possible physical processes involved in the emission of luminescence, but rather to provide some insight into the complex competition processes taking place in the quartz samples.

Fig. 9 shows a schematic diagram of the model comprising the main OSL trap and three luminescence centres L1, L2, L3. The set of differential equations that describe the various charge movements during the stimulation pulse is:

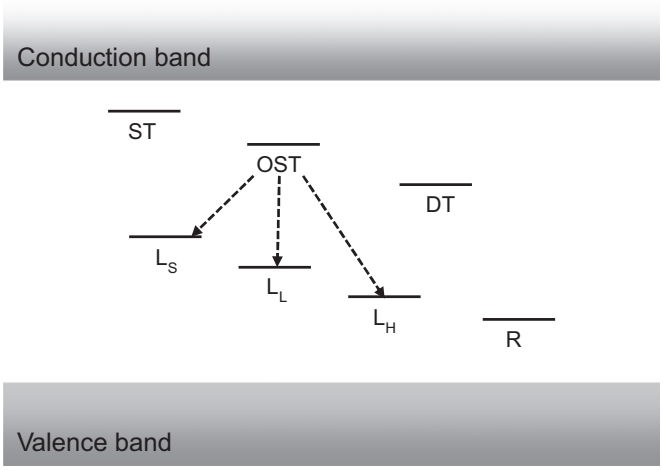

Fig. 8. The energy band model used to discuss luminescence lifetimes. Luminescence centres are shown as L_H, L_L and L_S. and the non-radiative centre as R. ST denotes shallow electron traps; OST, optically sensitive traps and DT stands for deep traps which are not optically stimulated.

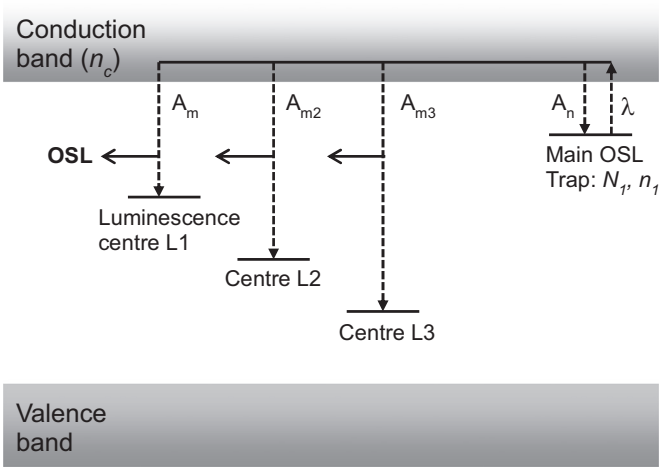

Fig. 9. The energy levels in the kinetic model for quartz, consisting of a single electron trap (Main OSL trap) and three recombination centres L1, L2 and L3 (reproduced from Pagonis et al. [16]).

$$\frac{dn_1}{dt} = -\lambda n_1(t) + A_n(N_1 - n_1(t))n_c(t) \tag{8}$$

$$\frac{dm_1}{dt} = -A_{m1}m_1(t)n_c(t) \tag{9}$$

$$\frac{dm_2}{dt} = -A_{m2}m_2(t)n_c(t) \tag{10}$$

$$\frac{dm_3}{dt} = -A_{m3}m_3(t)n_c(t) \tag{11}$$

$$\frac{dn_c}{dt} = \frac{dm_1}{dt} + \frac{dm_2}{dt} + \frac{dm_3}{dt} - \frac{dn_1}{dt} \tag{12}$$

The instantaneous luminescence is defined as

$$L = -\frac{dm_1}{dt} - \frac{dm_2}{dt} - \frac{dm_3}{dt} \quad . \tag{13}$$

After the LED pulse is turned off, the system of equations remains the same, except that Eq. (8) is changed by setting the constant λ to zero,

$$\frac{dn_1}{dt} = A_n(N_1 - n_1(t))n_c(t) \tag{14}$$

In the equations above and in Fig. 9, N_1 and n_1 are the total and instantaneous concentrations of the electron trap, and m_1, m_2, m_3 are corresponding instantaneous concentrations of the three recombination centres L1, L2, L3 and n_c is the concentration of electrons in the conduction band. The constant λ is given by $\lambda = \sigma I_o$ (s^{-1}) where σ is the photoionization cross section and I_o represents the intensity of the stimulating light. The first term $-\lambda n_1(t)$ in Eq. (8) expresses the optical excitation of the electrons out of the trap, while the second term $A_n(N_1 - n_1(t))$ expresses the possibility of retrapping of electrons with probability A_n. Here A_{m1}, A_{m2} and A_{m3} are the probabilities of capturing electrons from the conduction band into the recombination centres. Eq. (12) expresses the conservation of charge in the system and Eq. (13) is based on the assumption that all three recombination centres contribute to the observed pulsed OSL signal. This assumption is consistent with the qualitative models suggested by Chithambo et al. [13] and Ogundare et al. [38]. The implicit assumption in Eq. (13) is that all three transitions have the same efficiency and that all photons from the three recombination centres are detected, even though they correspond most likely to different energies. In general, one would have to multiply each term in Eq. (13) with an appropriate efficiency factor.

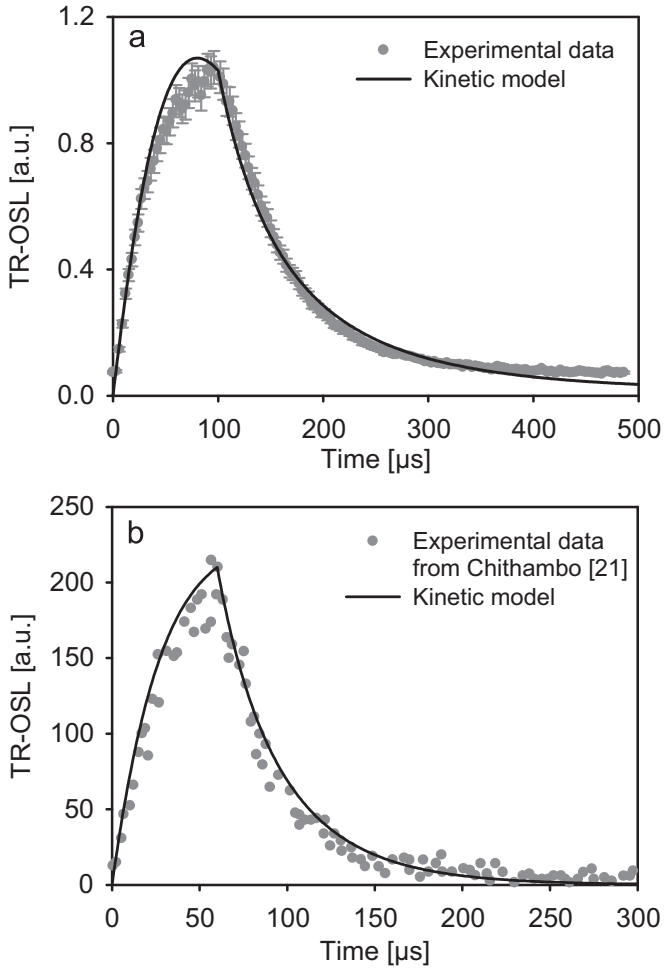

Fig. 10. (a) Comparison of the simulation results from the kinetic model for quartz with the experimental data. (b) Comparison of the simulation results for another set of parameters with the published experimental data [21]. All parameters used in the model are given in the text (reproduced from Pagonis et al. [16]).

Fig. 10 shows the results of simulation using the following set of parameters: $N_1 = 10^9$ cm^{-3}; $n_{10} = 10^9$ cm^{-3}; $A_n = 8 \times 10^{-6}$ cm^3 s^{-1}; $m_{10} = 9 \times 10^7$ cm^{-3}; $m_{20} = 0$; $m_{30} = 0$; $A_{m1} = 1.75 \times 10^{-4}$ cm^3 s^{-1}; $A_{m2} = 0$; $A_{m3} = 0$; $\lambda = 10^3$ s^{-1}. It is noted that the centres L2 and L3 play no role in this simulation, since A_{m2} and A_{m3} are set equal to zero. Here n_{10} and m_{10} are the initial concentrations of electrons and holes in the main trap and luminescence centre respectively. Conservation of charge requires that the total concentrations of electrons and holes in the traps and centers should be equal. The values of n_{10} and m_{10} listed above are not; however, this does not represent an unrealistic physical situation. It is usual to assume in this type of kinetic model that additional free charges exist in other traps and/or recombination centres in the quartz sample, leading to an overall balance of charge. It is noted that the values of the parameters in this simulation are meant as examples, and their absolute values are rather arbitrary. For example, the normalised results of the simulation in Fig. 10 remain unchanged if all the retrapping and recombination coefficients are multiplied by a scaling factor (for example 0.01), while at the same time the concentrations of traps and centers are divided by the same scaling factor.

Fig. 10 (a) compares the results of the simulation with the experimental data for quartz [16]. Both the experimental data and the simulation results were normalised to aid visual comparison.

The error bar associated with each data point in Fig. 10 (a) is simply the square-root of each data point since the luminescence photons events are random.

Fig. 10 (b) shows the results of running the simulation with another set of parameters, that is, $N_1=10^9\ \mathrm{cm}^{-3}$; $n_{10}=10^9\ \mathrm{cm}^{-3}$; $A_n=8\times10^{-6}\ \mathrm{cm}^3\ \mathrm{s}^{-1}$; $m_{10}=5\times10^9\ \mathrm{cm}^{-3}$; $m_{20}=m_{30}=0$; $A_{m1}=6.1\times10^{-4}\ \mathrm{cm}^{-3}$; $A_{m2}=0$; $A_{m3}=0$; $\lambda=200\ \mathrm{s}^{-1}$. The results of this simulation are compared directly with the experimental data previously published by Chithambo [21]. The selected examples shown in Fig. 10 demonstrate that the kinetic model presented in this section successfully simulates the typical experimental behaviour of quartz under pulsed optical stimulation. Pagonis et al. [16] also presented examples of non-monotonic behaviour of the pulsed-OSL signal from quartz.

The simulations in Fig. 10 are of course a simplification of a much more complex situation. In principle these simulations should also include the irradiation and relaxation periods which precede the TR-OSL experiment and one should not in principle assign random initial charges to the traps and the centers in the simulations. However, these simplified simulations serve as a first attempt at describing these TR-OSL signals, both during optical stimulation and during the relaxation periods. A more complete description must include the irradiation and relaxation periods preceding the TR-OSL experiment.

5.3. Analytical expressions for thermal quenching effects on time-resolved OSL signals from quartz

Pagonis et al. [39] presented a numerical kinetic model for thermal quenching in quartz, based on the well-known Mott–Seitz mechanism (see for example Bøtter-Jensen et al., [40], page 44). Fig. 11 shows schematic diagrams to explain thermal quenching in the model of Pagonis et al. [39]. The Mott-Seitz mechanism is shown schematically using a configurational coordinate diagram in Fig. 11(a), and consists of an excited state of the recombination centre and the corresponding ground state. Electrons are captured into the excited state, from which they can undergo either a direct radiative recombination resulting in the emission of light, (shown as a vertical dashed arrow in Fig. 11(a), or an indirect thermally assisted non-radiative transition into the ground state of the recombination centre. The activation energy ΔE for this non-radiative process is also shown in Fig. 11(a), and is an important experimentally determined parameter. The thermal quenching model of Pagonis et al. [39] is shown schematically in Fig. 11(b), and consists of the dosimetric electron trap shown as level 1, and three levels labelled 2–4 representing energy states within the recombination centre. During transition 1 in Fig. 11(b), electrons from the dosimetric trap are raised by optical stimulation into the conduction band (CB), with some of these electrons being re-trapped via transition 2 with a probability A_n. Transition 3 corresponds to an electronic transition from the CB into the excited state located below the conduction band with probability A_{CB}, while transition 5 indicates the direct radiative transition from the excited level into the ground electronic state with probability A_R, and transition 4 indicates the competing thermally assisted route. The probability for this competing thermally assisted process is given by a Boltzmann factor of the form $A_{NR}\exp(-\Delta E/kT)$ where ΔE represents the activation energy for this process and A_{NR} is a constant representing the non-radiative transition probability. Transition 6 denotes the non-radiative process into the ground state, and thermal quenching is determined by the ratio of the non-radiative and radiative probabilities A_{NR}/A_R and the value of the thermal activation energy. As the temperature of the sample is increased, electrons are removed from the excited state according to the Boltzmann factor and this leads to both a decrease of the intensity of the luminescence signal and to a simultaneous

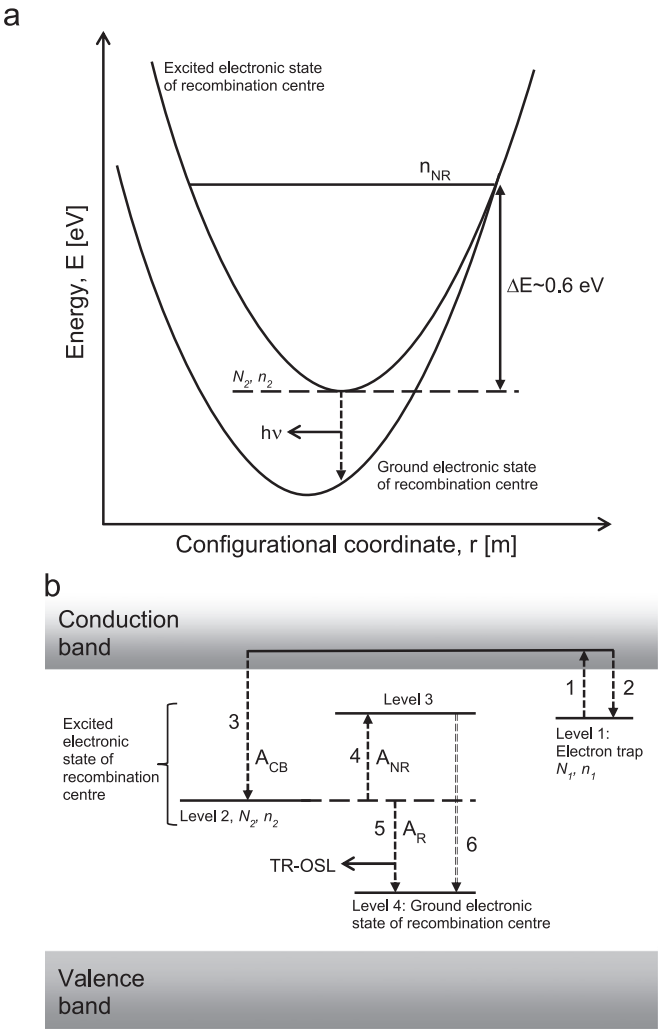

Fig. 11. (a) The configurational coordinate diagram for quartz, based on the Mott–Seitz mechanism of thermal quenching. (b) The kinetic model of Pagonis et al. [39] to explain thermal quenching in quartz, based on the Mott–Seitz mechanism.

apparent decrease of the luminescence lifetime.

The parameters used in the model are: N_1 is the concentration of dosimetric traps (cm^{-3}), n_1 is the corresponding concentration of trapped electrons (cm^{-3}), N_2 and n_2 are the concentrations of electron traps and filled traps correspondingly in the excited level 2 of the recombination centre (cm^{-3}), $\Delta E=0.64$ eV is the activation energy for the thermally assisted process (eV), A_n is the conduction band to electron trap transition probability coefficient ($\mathrm{m}^3\ \mathrm{s}^{-1}$), A_R and A_{NR} are the radiative and non-radiative transition probability coefficients (s^{-1}), and A_{CB} is the transition probability coefficient ($\mathrm{cm}^3\ \mathrm{s}^{-1}$) for the conduction band to excited state transition. The parameter n_c represents the instantaneous concentration of electrons in the conduction band (cm^{-3}) and f denotes the probability of optical excitation of electrons from the dosimetric trap (s^{-1}). Pagonis et al. [39] found good quantitative agreement between the model and experimental data obtained using a single-aliquot procedure on a sedimentary quartz sample (WIDG8). The sample WIDG8 has been used in the development of the single aliquot regenerative-dose (SAR) protocol, as well as for various luminescence characteristics studies (Wintle and Murray [41] and references within).

The mathematical aspects of the model of Pagonis et al. [39] were considered also in detail by Pagonis et al. [42] who developed analytical expressions for the TR-OSL intensity observed during and after a TR-OSL pulse in quartz experiments:

$$I(t) = A_R \frac{f}{A_R + A_{NR}\exp(-\Delta E/kT)}\left(1 - e^{-[A_R + A_{NR}\exp(-\Delta E/kT)]t}\right) \quad \text{for } 0 < t < t_w \text{ (DURING PULSE)} \tag{15}$$

$$I(t) = A_R n_2(t_w) e^{-[A_R + A_{NR}\exp(-\Delta E/kT)](t - t_w)} \quad \text{for } t > t_w \text{ (AFTER PULSE)} \tag{16}$$

where t_w represents the pulse width. These two equations agree with experimental results showing that the TR-OSL intensity for quartz during the stimulating light pulse can be described as a saturating exponential, while $I(t)$ after the stimulation light pulse is found to be a decaying simple exponential function. From the last two equations one finds the relaxation time for electrons from the excited into the ground state of the recombination centre:

$$\tau = \frac{1/A_R}{1 + \frac{A_{NR}}{A_R}\exp(-\Delta E/kT)} \tag{17}$$

This expression is of the same form as Eq. (4) in Section 4.1 of this paper. Another important result from the model is the following analytical expression for the maximum intensity during the optical pulse:

$$I_{max} = \frac{f}{1 + \frac{(A_{NR})}{A_R}\exp(-\Delta E/kT)} \tag{18}$$

which has the same mathematical form as Eq. (7) in this paper.

Pagonis et al. [42] also developed analytical expressions for the concentration of electrons in the conduction band during and after the TR-OSL pulse, and showed that their analytical expressions are equivalent to previous analytical expressions derived by Chithambo [21, 25], as described in Section 3.1 of this paper. These authors also presented a detailed description of thermal quenching processes in quartz based on AlO_4 defects, and discussed the various descriptions of the luminescence process in quartz found in the literature.

In a later comprehensive experimental and modelling work, Pagonis et al. [43] extended their analytical model for thermal quenching in quartz to annealed quartz samples, by including two luminescence centres L_H and L_L, as well as a hole reservoir R. This energy scheme is very similar to the one shown in Fig. 8 of this paper. The new extended model is also based on the Mott–Seitz mechanism of thermal quenching, and on a system of differential equations describing localised electronic transitions between energy states *within* the two luminescence centres. These authors showed that using simplifying physical assumptions leads to analytical solutions for the intensity of the light during a TR-OSL experiment with previously annealed samples. These analytical expressions were shown to be in quantitative agreement with published experimental data for commercially available quartz samples. Specifically the model describes the variation of the luminescence lifetimes with (a) annealing temperatures between room temperature and 900 °C (Fig. 6), and (b) with stimulation temperatures between 20 and 200 °C (Fig. 5).

Pagonis et al. [43] also reported on new detailed radioluminescence (RL) measurements carried out using the same commercially available quartz samples. These new experimental RL results were discussed within the context of their model. The change in luminescence lifetimes caused by annealing reported Galloway [10] and modelled by Pagonis et al. [43] necessarily implies that the emission wavelength corresponding to particular annealing temperatures should differ. Since it is measured as a function of the emission wavelength, RL was used to investigate whether annealing does indeed cause changes in the luminescence emission bands and to assess whether these changes can be correlated with the corresponding effect of annealing on lifetimes. It was concluded that changes in the position and intensities of RL emission bands observed were correlated with annealing up to 1000 °C.

6. Applications

Since the initial study on natural materials by Sanderson and Clark [2] using pulsed blue light to stimulate feldspar, the utility of time-resolved OSL has not been limited to studies on the physical processes of luminescence, but has been demonstrated in several different applications. Those relevant for quartz are summarized in this section.

6.1. Pulsed stimulation for the separation of quartz luminescence in the presence of feldspar

6.1.1. Basics of pulsed separation

Quartz is widely used for applications within accident dosimetry and dating geological or archaeological material, but as quartz and feldspar record different doses due to an additional internal dose rate in feldspar from ^{40}K, it is important to separate the signal from these two minerals to obtain the correct age [17, 18, 44]. However, in some samples feldspar inclusions within quartz grains prohibit complete physical separation even following chemical treatment, and instrumental separation is more appropriate. By utilising the difference in shape between TR-OSL spectra from quartz and feldspar during blue or green light stimulation [1, 2, 9, 17, 45–48], it is possible to obtain a quartz dominated luminescence signal from a sample with irremovable feldspar contamination. This is illustrated in Fig. 12(a), comparing the TR-OSL from quartz and feldspar following a 40 μs blue stimulation pulse (dashed line). The feldspar signal (grey full line) is dominated by <1 μs lifetime components while the quartz signal (black full line) is dominated by a $\sim$30 μs lifetime. The TR-OSL from a mixed sample will contain both signals (Fig. 12(b)), and a quartz dominated luminescence signal can be obtained by gating the PMT signal to omit the first few μs in the off-time (dominated by the feldspar signal), and only record the following luminescence signal.

The applicability of this approach was initially demonstrated in a laboratory experiment where a quartz dose was accurately determined in the presence of up to 40% feldspar contamination (by mass) [17, 18], and confirmed by another study estimating quartz doses from 11 natural fluvial samples with no prior chemical treatment [44]. Optimisation of the pulse duration and delay allowed further improvement of the separation between the signals and an enhancement of luminescence from dim samples [47], and additional natural measurements demonstrated the potential usefulness of pulsed separation for screening untreated samples in the field using a portable instrument [48]. Although no pulsed measurements of dose undertaken in the field have been published so far, several studies have used this technique to date quartz samples with irremovable feldspar contamination. The sections below discuss these applications based on the origin of the quartz, whether it is extracted from a variety of sediments or rock as the material properties are often dependent on the source. To conclude, there is a section on application to retrospective dosimetry, which is becoming increasingly important.

6.1.2. Applications of pulsed signal separation to sediments

The first application study used pulsed stimulation for quartz signal separation on two fluvial samples (out of nine) from an aeolian and fluvial sediment core drilled into the Heidelberg basin (Germany), altogether providing a chronology suggesting fluvial

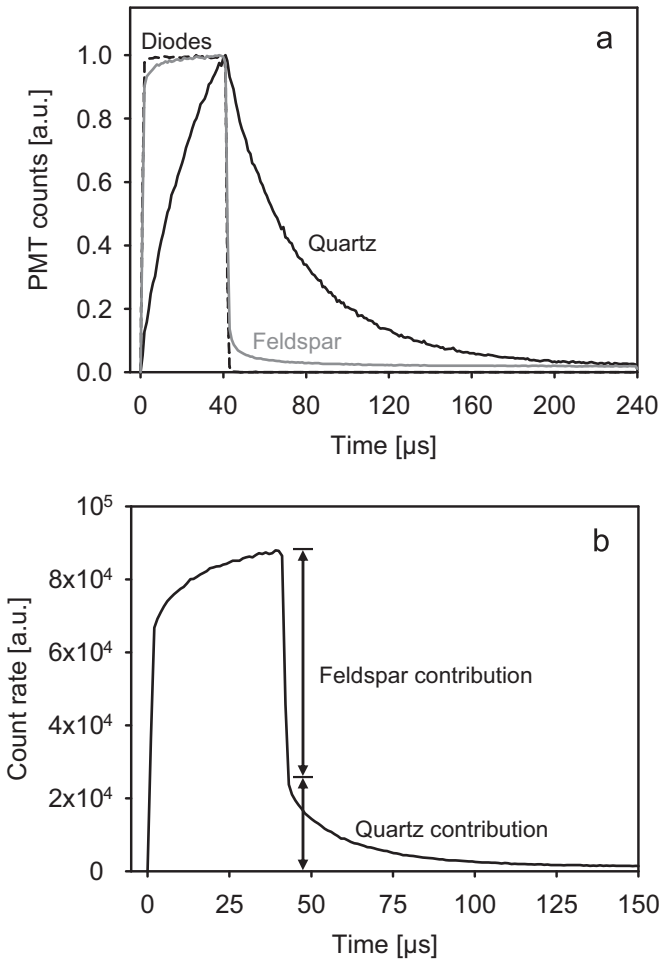

Fig. 12. (a) Time-resolved responses of both quartz and feldspar using pulsed stimulation with a pulse of 40 μs, and an off-time of 200 μs. The results have been integrated over the 5×10^5 pulses delivered during the 110 s stimulation, and normalised for ease of comparison. The dotted line shows the shape of the blue stimulation LED pulse. (b) Time-resolved response from a mixed quartz–feldspar sample following a pulse of 40 μs. Both redrawn after Denby et al. [17].

deposition during the Weichselian and coversand deposition at 9–11 ka [49]. A different study by the same lead author [50] collected two fluvial samples from a construction site in Cologne exposing Roman time harbour sediments of which one quartz sample was contaminated with feldspar and measured using pulsed OSL. Indications suggest that this sample was incompletely bleached, but no direct age control was available to evaluate the POSL age. The OSL age from the non-contaminated sample was analysed using different statistical models which overall agree with the age-bracket of 2080 ± 85–2010 ± 55 years BP provided by radiocarbon [50]. The question of incompletely bleached fluvial sediment is tackled in a different study by dating both the quartz and feldspar fractions in eight out of nine samples from the Lake Karakul basin in Tajikistan [51]. The authors conclude that the agreement between the quartz pulsed OSL and K-feldspar post-IR IRSL at 290 °C ($pIRIR_{290}$) ages confirm that the samples were adequately reset in nature.

Compared to fluvial samples, coastal sediments are often more well-bleached as in these two studies from beaches in Sardinia [52] and Taiwan [53]. The first study collected nine samples from five sites along the coast of Sardinia and found that four of the samples contained irremovable contamination and were dated using POSL. The quartz POSL and OSL ages broadly agree with feldspar post-IR $IRSL_{225}$ ages from the same samples, suggesting the sites formed prior to and during MIS 5, but ultimately being inconclusive as the ages are not in agreement with Late Würmian and Holocene radiocarbon ages from three of the sites [52]. The second coastal study obtained 17 samples from the Fulong beach in Taiwan and measured all with POSL, currently comprising the largest study utilising pulsing for dating of quartz. The ages span from initialisation of sediment accumulation at Fulong beach at about 5130 ± 360 years ago till dune ridge formation as recent as 60 ± 20 years ago [53].

Polymineral fine grained (4–11 μm) sediment is impossible to split into separate quartz and a feldspar fractions, therefore quartz extracts are often obtained by etching the sample until the feldspar is removed which is not always ideal [54], and an alternative is pulsed stimulation of the polymineral fine grained samples to obtain a quartz signal. This is demonstrated by Feathers et al. [55] where nine polymineral fine-grained samples from artefact bearing terraces in Jiuzhaigou National Park (China) was measured using POSL and OSL (both with an infrared prior-IR stimulation prior to the measurement to eliminate the feldspar signal). Although the POSL is shown to remove a fading component present in the OSL ages, the samples are poorly bleached and the ages might not represent the original aeolian deposition. In a different study by Tsukamoto and Kataoka [56] on volcanogenic outburst flood sediments from the Aso volcano (Japan), seven samples of polymineral tephric fine grained loess were all dated with POSL and $pIRIR_{290}$, agreeing within uncertainty for the four upper samples in the section to range from ~18–19 ka up to ~48–50 ka. However, the ages from the three lowermost samples are less in agreement; the bottom sample perhaps unsuitable for pulsed dating as the POSL signal is very dim, indicating a low quartz content. The corresponding $pIRIR_{290}$ age of 72 ± 6 ka is considered the best minimum age for this sample [56].

6.1.3. *Applications of pulsed signal separation to rocks*

Perhaps the most difficult category of quartz samples for luminescence dating originates from crystalline bedrock as they often exhibit high ratios of infrared to blue stimulated luminescence (indicating feldspar contamination), an insensitive OSL signal, and anomalously short recombination lifetimes during TR-OSL [57]. Nevertheless, Sohbati et al. [58] used pulsed stimulation to extract quartz dominated luminescence signals from rock slices cut from 5 quartzite cobbles sampled at an archaeological site in Portugal. The authors demonstrated that prolonged light exposure periods can create a distinct bleaching record in the dose depth profile into a cobble and that dating of multiple deposition (bleaching) events is possible in one sample; specifically for the archaeological site, two subsequent burial events at ~45 ka and ~20 ka were detected [58].

6.1.4. *Applications of pulsed signal separation in retrospective dosimetry*

Following a radiation accident, an assessment of the magnitude and extent of the damage is often required with urgency. Therefore, fast screening of radiation doses to natural dosimeters in the environment is vital, and provides the topic of two recent studies investigating building materials [59] and surface soils [60]. The first study investigates core disc samples from heated red brick, roof tile, ceramic tile, and toilet porcelain, all materials available in modern buildings. The validity of a pulsed OSL single aliquot additive dose method is demonstrated on a variety of samples, estimating doses of up to 7 Gy and with a minimum detection limit of 0.01 Gy. Furthermore, the time from sample preparation to dose estimation is estimated to about 2 ours as no chemical treatment was needed [59]. The second study investigates a pulsed OSL protocol for measuring a known irradiation dose of 4.3 Gy delivered to a Japanese surface soil and successfully recovers a dose of 4.9 ± 1.3 Gy using three aliquots [60]. Although further research is

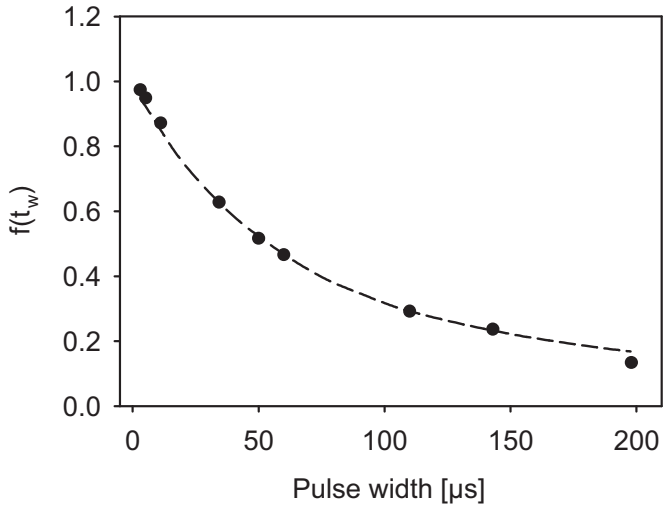

Fig. 13. The amount of luminescence measured after the light pulse as a proportion of the total measured signal plotted against the pulse width. Measurements were made on quartz annealed at 800 °C for 30 min and irradiated to 102 Gy before pulsed stimulation at 525 nm. The dashed line is the best fit of Eq. (19) (reproduced from [20]).

needed into different types of soil and building materials, the method of POSL seems very promising for fast dose screening [59, 60].

6.2. Dynamic throughput

The influence of the pulse width on the amount of luminescence that can be stimulated from a quartz sample of lifetime τ can be quantified as

$$f(t_w) = \frac{\tau}{t_w}(1 - \exp(-t_w/\tau)) \tag{19}$$

where t_w is the pulse width and the function $f(t_w)$ is the dynamic throughput [21, 25]. Eq. (19), in which the only variable is the pulse width t_w, gives the amount of luminescence measured after the light pulse as a proportion of the total measured signal. The dynamic throughput function has two possible applications, one concerning the luminescence intensity and the other to do with lifetime calculations. It can be deduced from Eq. (19) that the amount of luminescence that can be measured after the light pulse from a given sample can be increased if the pulse width is set to be a small fraction of the lifetime as is evident in Fig. 13. The same figure also provides a means to evaluate the lifetime if the luminescence intensity makes the use of related equations, e.g. (2) and (3), impractical.

7. Outlook

We have reviewed some important developments in time-resolved optical stimulation that have aided the understanding of mechanisms of luminescence from quartz in the last two decades. As one looks back at the advancements, it is opportune to contemplate areas where further research may refine our understanding of the dynamics of luminescence in quartz and possibly address outstanding problems in its applications. Of the many possible areas for further exploration, we would like to highlight three, namely, further work to make dating more precise and accurate, improvements in instrumentation to better exploit the possibilities that asynchronous stimulation and emission offers, and spectral measurements to investigate theories of luminescence lifetimes and recombination centres more effectively.

Regarding dating applications, several new techniques have been investigated in order to overcome the current age limit of ~150 to 250 ka for quartz OSL dating [61], and include quite different signals, such as the isothermal TL (ITL) signal (e.g. [62]) and the thermally transferred OSL (TT-OSL) signal ([63] and references therein). More recently, quartz characterisation and ages obtained using violet stimulated luminescence (VSL) yielded very optimistic results, indicating that the VSL signal accesses a deep trap that could extend the dating range [64], but different quartz samples with independent age control (1.6–0.7 Ma) yielded VSL ages underestimating the known ages [65]. To investigate the origin of these age underestimates, time-resolved VSL measurements contrasted with exo-electron measurements [66] or time-resolved exo-electron measurements [67] would provide insight into the charge movement in quartz during violet stimulation, and help improve the method. Since the time-resolved exo-electron signal can be measured simultaneously with the time-resolved luminescence signal and counts the amount of electrons escaping the crystal during and after optical stimulation, this records not only the electronic behaviour when escaping the dosimetric trap and transitions through the conduction band, but also the behaviour of the recombination centre emitting luminescence. Together these measurements provide unique snapshots in time that can map the migration of electrons through the crystal, and since the search for quartz signals that can extend the age range takes place in many laboratories worldwide, not only is violet stimulation of interest for further exploration, but other wavelengths are worth investigating in pursuit of overcoming current limitations and further improving the precision and accuracy of luminescence dating.

The extent to which developments in instrumentation for TR-OSL lags the ideals of Sanderson and Clark [2] is evident when one compares the concepts outlined in that paper with what has been achieved since. These authors singled out some benefits of pulsed OSL over continuous stimulation namely better signal-to-noise ratio, ability to measure time-scales and processes of recombination and, the possibility of detecting luminescence in cases where the stimulation wavelength overlaps with or is close to the emission wavelength. Whereas systems in use have demonstrated enhanced signal-to-noise ratio e.g [1], and sections 3 through 5 in this paper exemplify efforts at study of dynamics of luminescence, asynchronous measurement of luminescence where the emission and stimulation bands overlap is yet to be realised. This would offer advantages of use of a greater range of stimulation wavelengths than has perhaps been possible. This is because the set-up in contemporary instrumentation where band-pass filters are needed to transmit the luminescence and long-pass filters required to restrict the wavelength range of the luminescence stimulating light to avoid adversely affecting the signal-to-background ratio, in principle limit the range of stimulation wavelengths than can be used for a material emitting at a particular wavelength.

Our final proposal for future work concerns the need for measurement of emission spectra during OSL measurements. As has been demonstrated in thermoluminescence [68–70], spectral measurements provide a means to distinguish emission from different recombination centres. Although in the context of TR-OSL from quartz, efforts to correlate annealing and change in emission bands have been carried out using radioluminescence [43], such changes in emission bands can be directly revealed by the way of 3-D isometric plots of the intensity as a function of the measurement temperature and emission wavelength or as 2-D contour maps of wavelength and measurement temperature.

In principle, one can formulate many more areas for future research in TR-OSL on quartz. The examples discussed above are a few drawn from our experience on quartz and are not meant to be an exhaustive list of possibilities.

8. Summary

Time-resolved optical stimulation of luminescence has become established as a key method for measurement of optically stimulated luminescence in addition to steady-state methods discussed extensively elsewhere [40, 71, 72]. Although time-resolved optical stimulation has been used to study a wide variety of natural materials such as quartz [9–19, 21, 24, 25, 57], feldspar [1, 2, 17, 46, 47] and zircon [73] as well as synthetic ones such as α-Al_2O_3:C [3–6, 74] and BeO [75, 76]; for illustrative purposes this report is limited to studies on quartz with selected few applications drawn from studies also including feldspar. Time-resolved optical stimulation has been successfully applied to study the mechanism in the processes leading up to luminescence emission and is generating increased interest in retrospective dosimetry applications. The main means for investigation of dynamics has been the dependence of the intensity as well as the luminescence lifetime determined from time-resolved luminescence spectra on temperature. In this paper we have reviewed some key developments in theory and applications of the method including methods for evaluating lifetimes, techniques for evaluating kinetic parameters using both the dependence of luminescence intensity and lifetime on measurement temperature, and of lifetimes on annealing temperature. The paper also provides an overview of some selected applications such as the separation of component signals from a quartz–feldspar admixture and the utility of the dynamic throughput, a measure of luminescence measured as a function of the pulse width. In looking forward to many possibilities available in work on TR-OSL, we have made a few suggestions on areas where further enquiry may help address some outstanding problems in time-resolved optical stimulation of luminescence from quartz.

Acknowledgements

Makaiko Chithambo acknowledges with gratitude financial support from Rhodes University and the National Research Foundation of South Africa (Incentive Funding Grant IFR2010042300003). CA is funded by Netherlands Organisation for Scientific Research, NWO VENI (Grant 863.13.023).

References

[1] M.L. Chithambo, R.B. Galloway, Meas. Sci. Technol. 11 (2000) 418.
[2] D.C.W. Sanderson, R.J. Clark, Radiat. Meas. 23 (1994) 633.
[3] B.G. Markey, L.E. Colyott, S.W.S. McKeever, Radiat. Meas. 24 (1995) 457.
[4] S.W.S. McKeever, M.S. Akselrod, B.G. Markey, Radiat. Prot. Dosim. 65 (1996) 267.
[5] E. Bulur, H.Y. Göksu, Radiat. Meas. 27 (1997) 479.
[6] E. Bulur E, H.Y. Göksu, W. Wahl, Radiat. Meas. 29 (1998) 625.
[7] R.J. Clark, L.K. Bailiff, M.J. Tooley, Radiat. Meas. 27 (1997) 211.
[8] R.J. Clark, I.K. Bailiff, Radiat. Meas. 29 (1998) 553.
[9] I.K. Bailiff, Radiat. Meas. 32 (2000) 401.
[10] R.B. Galloway, Radiat. Meas. 35 (2002) 67.
[11] M.L. Chithambo, F.O. Ogundare, Phys. Status Solidi (C) 4 (2007) 914.
[12] M.L. Chithambo, F.O. Ogundare, J. Feathers, Radiat. Meas. 43 (2008) 1.
[13] M.L. Chithambo, F. Preusser, K. Ramseyer, F.O. Ogundare, Radiat. Meas. 42 (2007) 205.
[14] M.L. Chithambo, Radiat. Meas. 37 (2003) 167.
[15] M.L. Chithambo, F.O. Ogundare, Radiat. Meas. 44 (2009) 453.
[16] V. Pagonis, S.M. Mian, M.L. Chithambo, E. Christensen, C. Barnold., J. Phys. D.: Appl. Phys. 42 (2009) 055407.
[17] P.M. Denby, L. Bøtter-Jensen, A.S. Murray, K.J. Thomsen, P. Moska, Radiat. Meas. 41 (2006) 774.
[18] K.J. Thomsen, L. Bøtter-Jensen, P.M. Denby, P. Moska, A.S. Murray, Radiat. Meas. 41 (2006) 768.
[19] M.L. Chithambo, Ancient TL 23 (2005) 39.
[20] M.L. Chithambo, J. Lumin. 131 (2011) 92.
[21] M.L. Chithambo, J. Phys. D: Appl. Phys. 40 (2007)1880 40 (2007).
[22] W. Becker, Advanced Time-Correlated Single Photon Counting Techniques, Springer-Verlag, Berlin, 2005.
[23] W. Becker, H. Hickl, C. Zander, K.H. Drexhage, M. Sauer, S. Siebert, J. Wolfrum, Rev Sci. Instrum. 70 (1999) 1835.
[24] T. Lapp, M. Jain, C. Ankjærgaard, L. Pirtzel, Radiat. Meas. 44 (2009) 571.
[25] M.L. Chithambo, J. Phys. D.: Appl. Phys. 40 (2007) 1874.
[26] S.W.S. McKeever, R. Chen, Radiat. Meas. 27 (1997) 625.
[27] R. Chen, P.L. Leung, Radiat. Meas. 37 (2002) 519.
[28] M.L. Chithambo, R.B. Galloway, Nucl. Instrum. Methods B 183 (2001) 358.
[29] F. Agullo–Lopez, C.R.A. Catlow, P.D. Townsend, Point Defects in Materials, Academic Press, London, 1988.
[30] A.G. Wintle, Geophys. J. R. Astron. Soc. 41 (1975) 107.
[31] S.A. Petrov, Bailiff, Radiat. Meas. 27 (1997) 185.
[32] R.M. Bailey, Radiat. Meas. 32 (2000) 233.
[33] L. Bøtter-Jensen, N. Agersnap Larsen, V. Mejdahl, N.R.J. Poolton, M.F. Morris, S. W.S. McKeever, Radiat. Meas. 24 (1995) 535.
[34] N.R.J. Poolton, G.M. Smith, P.C. Riedi, E. Bulur, L. Bøtter-Jensen, A.S. Murray, M. Adrian, J. Phys. D 33 (2000) 1007.
[35] S. Fleming, Thermoluminescence Techniques in Archaeology, Oxford University Press, UK, 1979.
[36] M.L. Chithambo, P. Sane, F. Tuomisto, Radiat. Meas. 46 (2011) 310.
[37] J. Zimmerman, J. Phys. C 4 (1971) 3265.
[38] F.O. Ogundare, M.L. Chithambo, Opt. Mater. 29 (2007) 1844.
[39] V. Pagonis, C. Ankjærgaard, A.S. Murray, M. Jain, R. Chen, J. Lawless, S. Greilich, J. Lumin. 130 (2010) 902.
[40] L. Bøtter-Jensen, S.W.S. McKeever, A.G. Wintle, Optically Stimulated Luminescence Dosimetry, Elsevier Science Publishers, Amsterdam, 2003.
[41] A.G. Wintle, A.S. Murray, Radiat. Meas., 41, (2006) 369.
[42] V. Pagonis, J. Lawless, R. Chen, M.L. Chithambo, J. Lumin. 131 (2011) 1827.
[43] V. Pagonis, M.L. Chithambo, R. Chen, A. Chruścińska, M. Fasoli, S.H. Li, M. Martini, K. Ramseyer, J. Lumin. 145 (2014) 38.
[44] K.J. Thomsen, M. Jain, A.S. Murray, P.M. Denby, N. Roy, L. Bøtter-Jensen, Radiat. Meas. 43 (2008) 752.
[45] I.K. Bailiff, V.B. Mikhailik, Radiat. Meas. 37 (2003) 151.
[46] C. Ankjærgaard, M. Jain, K.J. Thomsen, A.S. Murray, Radiat. Meas. 45 (2010) 778.
[47] C. Ankjærgaard, M. Jain, R. Kalchgruber, T. Lapp, D. Klein, S.W.S. McKeever, A. S. Murray, P. Morthekai, Radiat. Meas. 44 (2009) 576.
[48] H.M. Kook, A.S. Murray, T. Lapp, P.H. Denby, C. Ankjærgaard, K.H. Thomsen, M. Jain, J.H. Choi, G.H. Kim, Nucl. Instrum. Methods B 269 (2011) 1370.
[49] T. Lauer, M. Frechen, C. Hoselmann, S. Tsukamoto, Proc. Geol. Assoc. 121 (2010) 154.
[50] T. Lauer, R. Bonn, M. Frechen, M.C. Fuchs, M. Trier, S. Tsukamoto, Geochronometria 38 (2011) 341.
[51] T. Komatsu, S. Tsukamoto, Quarternary Res. 83 (2015) 137.
[52] C. Thiel, M. Coltorti, S. Tsukamoto, M. Frechen, Quat. Int. 222 (2010) 36.
[53] N. Dörschner, T. Reimann, D. Wenske, C. Lüthgens, S. Tsukamoto, M. Frechen, M. Böse, Quat. Int. 263 (2012) 3.
[54] B. Mauz, A. Lang, Ancient TL 22 (2004) 1.
[55] J.K. Feathers, M.A. Casson, A.H. Schmidt, M.L. Chithambo, Radiat. Meas., 47, (2012) 201.
[56] S. Tsukamoto, K.S. Kataoka, Y. Miyabuchi, Geochronometria 40 (2013) 294.
[57] B. Guralnik, C. Ankjærgaard, M. Jain, A.S. Murray, A. Müller, M. Wälle, S. E. Lowick, F. Preusser, E.J. Rhodes, T.-S. Wu, G. Mathew, F. Herman, Quatern. Geochronol. 25 (2015) 37.
[58] R. Sohbati, A.S. Murray, J.P. Buylaert, N.A. Almeida, P.P. Cunha, Boreas 41 (2012) 452.
[59] M.J. Kim, Y.J. Lee, J.I. Lee, J.L. Kim, D.G. Hong, Radiat. Meas. 71 (2014) 490.
[60] H. Fujita, Radiat. Phys. Chem. 104 (2014) 84.
[61] A.G. Wintle, Archaeometry 50 (2008) 276.
[62] M. Jain, L. Bøtter-Jensen, A.S. Murray, P.M. Denby, S. Tsukamoto, M.R. Gibling, Ancient TL 23 (2005) 9.
[63] G.A.T. Duller, A.G. Wintle, Quat. Geochronol. 7 (2012) 6.
[64] C. Ankjærgaard, M. Jain, J. Wallinga, Quat. Geochronol. 18 (2013) 99.
[65] C. Ankjærgaard, B. Guralnik, N. Porat, A. Heimann, M. Jain, M., J. Wallinga, Radiat. Meas. (2015), 10.1016/j.radmeas.2015.01.011 (in press).
[66] C. Ankjærgaard, P.M. Denby, A.S. Murray, M. Jain, Radiat. Meas. 43 (2008) 273.
[67] S. Tsukamoto, A.S. Murray, C. Ankjærgaard, M. Jain, T. Lapp, J. Phys. D: Appl. Phys. 43 (2010) 325502.
[68] P.D. Townsend, Y. Kirsh, Contemp. Phys. 30 (1989) 337.
[69] M.L. Chithambo, V. Pagonis, F.O. Ogundare, J. Lumin. 145 (2014) 180.
[70] M.L. Chithambo, A.N. Nyirenda, A.A. Finch, N.S. Rawat, N.S., Phys. B: Condens. Matter 473 (2015) 62.
[71] F. Preusser, M.L. Chithambo, T. Götte, M. Martini, K. Ramseyer, E.J. Sendezera, G.J. Susino, A.G. Wintle, Earth-Sci. Rev. 97 (2009) 196.
[72] M. Jain, J.H. Choi, P.J. Thomas, Radiat. Meas. 43 (2008) 709.
[73] E. Bulur, E. Kartal, B.E. Saraç, Radiat. Meas. 60 (2014) 46.
[74] V. Pagonis, C. Ankjærgaard, M. Jain, R. Chen, J. Lumin. 136 (2013) 270.
[75] E. Bulur, B.E. Saraç, Radiat. Meas. 59 (2013) 129.
[76] E. Bulur, Radiat. Meas. 66 (2014) 12.